ACES Asian Chemical Editorial Society

DOI: 10.1002/asia.201600434

CHEMISTRY AN ASIAN JOURNAL Full Paper

Coordination Polymers

Microcrystalline Zinc Coordination Polymers as Single-site Heterogeneous Catalysts for the Selective Synthesis of Mono-oxazolines from Amino Alcohol and Dinitriles

Junning Wang[+], Chao Huang[+], Kuan Gao, Xiaolu Wang, Mengjia Liu, Haoran Ma, Jie Wu,* and Hongwei Hou*[a]

Abstract: In our effort to develop coordination polymers (CPs)-based single-site catalysts for the selective synthesis of mono-oxazolines, two Zn-based CPs, $[\{Zn_6(idbt)_4(phen)_4\}\cdot 3H_2O]_n$ (**1**) and $[\{Zn_3(idbt)_2(H_2O)_4\}\cdot 2H_2O]_n$ (**2**) (H_3idbt = 5,5′-(1*H*-imidazole-4,5-diyl)-bis-(2*H*-tetrazole), phen = 1,10-phenanthroline) have been synthesized. They exhibit two-dimensional structure and contain isolated and accessible catalytically active sites, mimicking the site isolation of many catalytic enzymes. Micro CPs **1** and **2** are obtained by using surfactant-mediated hydrothermal methods, and an investigation is conducted to explore how different surfactants affect their morphologies and particle sizes. Furthermore, micro **1** and **2** have shown to be effective heterogeneous catalysts for the reaction of amino alcohols and aromatic dinitriles, and exerted a significant influence on the selectivity of the catalytic reactions, yielding mono-oxazolines as the major reaction product.

Introduction

Coordination polymers (CPs), including metal–organic frameworks (MOFs), have recently emerged as promising new materials for gas storage,[1–3] sensing,[4,5] drug delivery,[6] light harvesting,[7,8] heterogeneous catalysis.[9] In particular, CPs have been established as a highly tunable platform for developing immobilized well-defined molecular catalysts, leading to a new generation of solid catalysts with uniform catalytic sites for various reactions, such as aldol condensation,[10,11] C–C bond formations,[12,13] epoxidations,[14–16] oxidations,[17,18] cyclization,[19,20] fixed-bed reactions,[21] and so forth. In comparison with other immobilized systems, CPs have highly ordered crystalline structures, high catalyst loadings, more uniform and isolated catalytic sites, thus eliminating multimolecular catalyst deactivation pathways.[13] In addition, by scaling down the sizes of CPs into microregime, the formed microscale CPs as heterogeneous catalysts can usually exhibit unique and enhanced catalytic properties because they not only maintain the structural diversity and physicochemical properties as bulk phase CPs but also exhibit particle dimensions in the tens to hundreds of micrometers range, endowing them higher catalytic efficiency.

On the other hand, oxazoline derivatives exhibit various pharmaceutical activities, such as antidiabetic,[22] antihypertensive,[23] antidepressant,[24] anticancer,[25] and so forth. The tandem condensation–cyclodehydration reaction of amino alcohol and nitriles toward the synthesis of oxazoline derivatives is one of the most efficient methods.[26–28] However, the reaction of amino alcohols and dinitriles to selectively prepare mono-oxazolines is still a considerable challenge, because it usually affords a mixture of bis- and mono-oxazolines as co-products in the reported catalytic systems.[28–33] As a research program of our laboratory, we are interested in developing an approach to obtain mono-oxazolines by the reactions of amino alcohols and dinitriles, as there are possibilities to further elaborate the remaining nitrile function, such as tetrazole, carboxylic acid, and carboxylic acid derivatives. Encouraged by the merits of CPs-based heterogeneous single-site catalysts, we attempt to explore whether the CPs could selectively catalyze such reactions.

In this work, with a rigid and conjugated clamp-like ligand (H_3idbt), two zinc-based coordination polymers $[\{Zn_6(idbt)_4(phen)_4\}\cdot 3H_2O]_n$ (**1**) and $[\{Zn_3(idbt)_2(H_2O)_4\}\cdot 2H_2O]_n$ (**2**) have been synthesized. Furthermore, microscale CPs **1** and **2** were introduced with the addition of polyvinylpyrrolidone (PVP-1300 000), hexadecyltrimethylammonium bromide (CTAB), and sodium dodecyl sulfate (SDS) as surfactants for high dispersion of the catalyst in solution and more effective utilization of zinc catalytic sites. With the addition of micro CPs **1** (or **2**) as heterogeneous catalysts, mono-oxazolines as the major product were achieved by reacting amino alcohols with dini-

[a] J. Wang,[+] C. Huang,[+] K. Gao, X. Wang, M. Liu, H. Ma, Prof. J. Wu, Prof. H. Hou
College of Chemistry and Molecular Engineering
Zhengzhou University, Zhengzhou (China)
Fax: (+86) 371-67761744
E-mail: wujie@zzu.edu.cn
houhongw@zzu.edu.cn

[+] These authors contributed equally to the work.

Supporting information and the ORCID identification number(s) for the author(s) of this article can be found under http://dx.doi.org/10.1002/asia.201600434.

triles, due to their distinct isolated and accessible catalytically active sites. A mechanism for the catalytic reaction has been proposed. The influence of surfactants on the morphologies and particle sizes of CPs has been investigated.

Results and Discussion

Structure of $[\{Zn_6(idbt)_4(phen)_4\}\cdot 3H_2O]_n$ (1)

Single-crystal X-ray crystallography revealed that **1** crystallizes in the monoclinic space group and shows a 2D gridding-like structure containing an octanuclear Zn^{II} secondary building unit (SBU). Four imidazole groups of ligand H_3idbt bridge two Zn1 and two Zn3 to form a square-like tetranuclear Zn^{II} macrocycle as inwall of the SBU by the repeat of -[-Zn1-imidazole-Zn3-]- linkage, whereas two tetrazole groups of the ligand chelate Zn2 on four sides of the square to form another tetranuclear block (Figure 1 a). Zn2 ion adopts a tetrahedral geometry and can be used as an isolated and accessible active site due to its azimuth, configuration, and unsaturated metal center, whereas Zn1 and Zn3 can be regarded as catalytically inactive (Figure S1 in the SI). Eight symmetry-related Zn^{II} atoms are linked by four $idbt^{3-}$ groups to construct a $[Zn_8(idbt)_3]$ SBU, which is bridged together by Zn atoms to form a 2D infinite gridding-like structure (Figure 1 b).

Structure of $[\{Zn_3(idbt)_2(H_2O)_4\}\cdot 2H_2O]_n$ (2)

Complex **2** exhibits a 2D ladder-like structure, which crystallizes in the monoclinic system, space group $P2_1/c$. As shown in Figure 2 a, the asymmetric unit of **2** consists three crystallographically independent Zn^{II} ions, two $idbt^{3-}$ ligands, four coordinated water molecules, and two lattice water molecules, as confirmed by the charge balance and TGA (Figure S2 in the SI). The Zn1 ion is surrounded by three nitrogen atoms from two $idbt^{3-}$ ligands and one oxygen atom from one water molecule to furnish a distorted tetrahedral geometry. Zn2 ion possesses the typical five-coordinated trigonal bipyramid coordination geometry. Zn1 and Zn2 are bridged by $idbt^{3-}$ ligands to form a 2D layer containing grids running along the *a*-axis formed by four Zn as vertexes and four $idbt^{3-}$ ligands as edges (Figure 2 b). Zn3 stretches out from the layer and adopts distorted trigonal bipyramid geometry by coordinating with two nitrogen atoms from one $idbt^{3-}$ ligands as well as three oxygen atoms from three coordinated water molecules. The coordinated water molecules are good leaving groups, they may depart during the catalytic process, leaving unsaturated zinc sites to be exposed to dinitriles, which is beneficial for the catalytic processes.

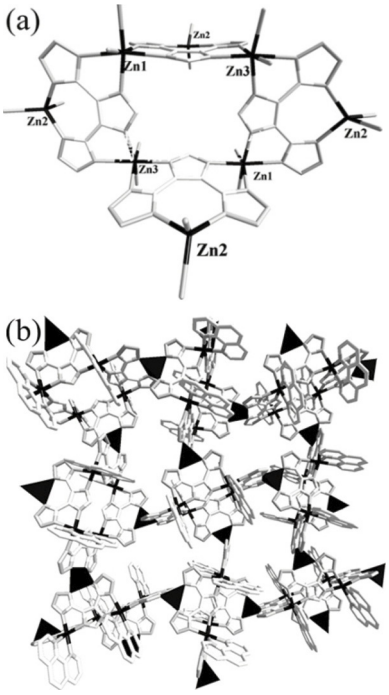

Figure 1. (a) View of the octanuclear in **1** (hydrogen atoms, free water molecule, and phen are omitted for clarity); atoms labelled white = carbon; black = zinc; gray(25 %) = nitrogen. (b) View of 2D layer structure of **1** along the *a*-axis (Zn atoms are shown in polyhedron).

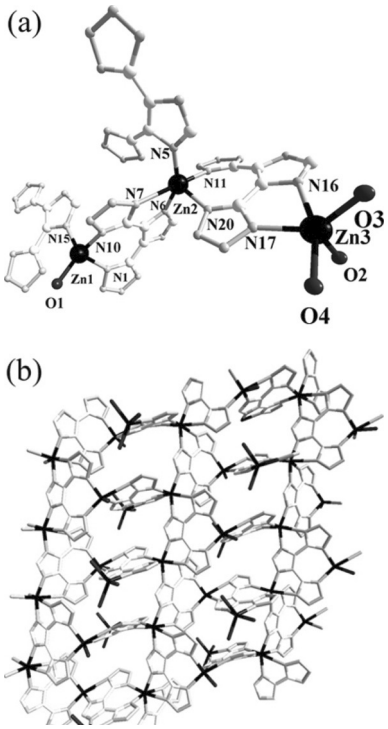

Figure 2. (a) The coordination environment of the Zn^{II} ions in **2** (Hydrogen atoms and free water molecule are omitted for clarity), atoms labelled white = carbon; black = zinc; gray(80 %) = oxygen; gray(25 %) = nitrogen; (b) the 2D layer structure viewed along the *a*-axis direction.

Dependence of surfactants on crystallite size and morphology

CPs have many advantages to be a kind of heterogeneous catalyst because of their large surface areas, isolated accessible active sites, and flexible and diverse structures. For a heterogeneous catalyst, deliberately scaling down the size of the catalyst and accessing a nanosized or microsized catalyst is an effi-

cient strategy to formulate materials with a high density of catalytically active sites.[34–37] Herein, several surfactants, such as PVP-1 300 000, CTAB, and SDS, were introduced individually into the hydrothermal reaction to construct catalysts with reduced size.

Without surfactants, cuboid crystals of **1** with dimensions of $\approx 0.3 \times 0.1 \times 0.1$ mm^3 were produced (Figure S3 in the SI). When PVP-1300 000 as a surfactant was added, the particle size of crystalline **1** was reduced drastically with narrow diameter distributions of nearly 8 μm in length and 500 nm in width (Figure 3 a). When CTAB was employed, the particle size could also be scaled down to the micrometer regime, and the average edge width of the resulting crystals is about 700 nm (Figure 3 b). In addition, crystals with an average edge width of 600 nm are obtained with SDS, as shown in Figure 3 c. Furthermore, with the addition of a surfactant (PVP, CTAB, or SDS) as

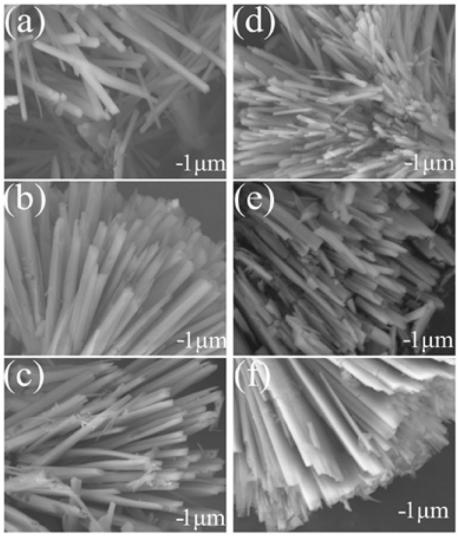

Figure 3. Scanning electron microscopy images of microcrystals: (a) microcrystals **1** with addition of PVP; (b) microcrystals **1** with addition of CTAB; (c) microcrystals **1** with addition of SDS; (d) microcrystals **2** with addition of PVP; (e) microcrystals **2** with addition of CTAB; (f) microcrystals **2** with addition of SDS.

template, microscale crystals of **2** could also be obtained through hydrothermal syntheses (Figure 3 d–f). Single crystals of **2** with edge width of about 0.08 mm were synthesized without surfactants (Figure S3 b in the SI). In contrast, with the addition of a surfactant (PVP, CTAB, or SDS), micro crystals of **2** with an average edge width of 600 nm were obtained.

In addition, powder X-ray diffraction (PXRD) analysis demonstrated that there is no significant change for the bulk phase and microscale crystals with the simulated of **1** and **2**, which indicated the microscale crystals are crystalline and have the same crystal structures as that of **1** and **2** (Figure 4). The surfactants could be served as capping agents to restrict the particle size, thus keeping the microcrystalline in micrometers along the width.[38,39]

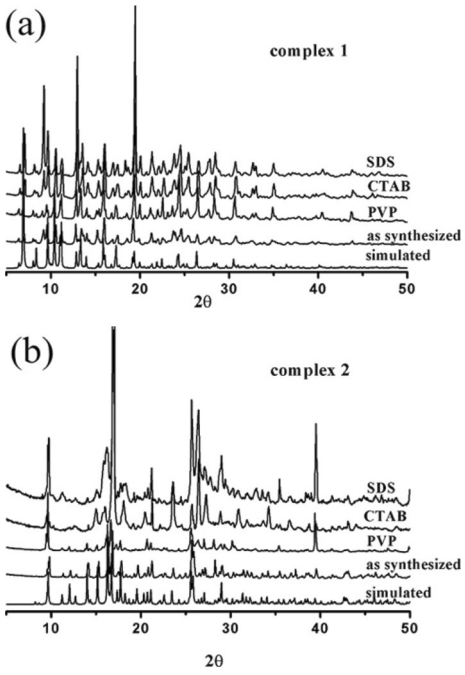

Figure 4. (a) Compared with different surfactants (PVP, CTAB, and SDS), experimental, and simulated PXRD patterns of complex **1**; (b) compared with different surfactants (PVP, CTAB, and SDS), experimental, and simulated PXRD patterns of complex **2**.

The concentration of the surfactants is another important factor, which determines the particle size and morphology of the product. The experiment was carried out under different concentrations of PVP-1 300 000, CTAB, or SDS (0.015, 0.025, 0.05, 0.075, 0.10, 0.125 and 0.15 g). A higher concentration of the reactant is considered to make ligands more likely to react with metal ions and the nucleation rate is faster, forming the smaller particles. Therefore, by increasing the concentration of the surfactants, the particle size becomes smaller. When the concentration of the surfactant was 0.15 g, the well-defined crystalline morphologies and particle sizes distributions of **1** and **2** could be obtained. Higher concentrations led to the formation of amorphous micro CPs rather than crystalline micro CPs. In addition, other surfactants, such as polyethylene glycol-20 000, sodium dodecylbenzenesulfonate, and polyethylene oxide, led to the formation of amorphous micro CPs rather than crystalline micro CPs.

The catalytic capacity of micro CPs 1 and 2

Oxazolines are ubiquitous in natural products and have been used for pharmaceutical drug discovery in recent years.[40–43] However, the design and synthesis of effective catalysts to selectively achieve mono-oxazolines from dinitriles still remains a challenge. The phase purity of the microcrystalline samples of **1**–**2** was determined by an excellent match between the microcrystalline and simulated PXRD patterns (Figure 4). To study the potentials of micro CPs of **1**–**2** as heterogeneous catalysts in the tandem condensation reaction of amino alcohols and dinitriles, their catalytic activities were initially evaluated with L-

Table 1. Catalyzed synthesis of mono-oxazolines from **4** with L-amino alcohol.[a]

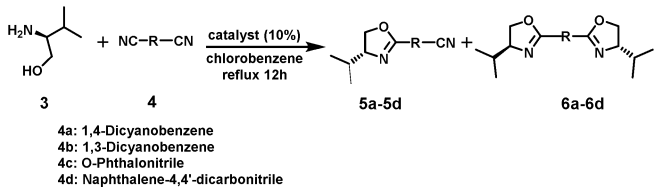

4a: 1,4-Dicyanobenzene
4b: 1,3-Dicyanobenzene
4c: O-Phthalonitrile
4d: Naphthalene-4,4'-dicarbonitrile

Entry	Catalyst	4	Yield [%] of **5a–d**[b]	Yield [%] of **6a–d**[b]
1	**1**	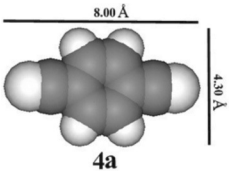	83	Trace
2	**2**		86	Trace
3	**1**	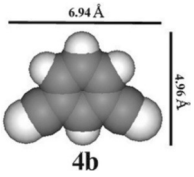	80	Trace
4	**2**		84	Trace
5	**1**	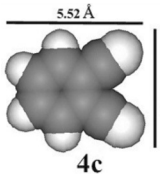	68	Trace
6	**2**		72	Trace
7	**1**	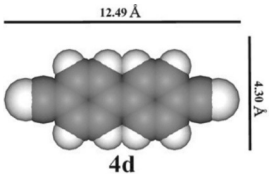	47	Trace
8	**2**		60	Trace

[a] Reaction conditions: L-aminoalcohols (3.0 mmol), aromatic dinitriles (1.0 mmol), catalyst (0.1 mmol), chlorobenzene (5 mL), 12 h. [b] Isolated yield of the product after 12 h.

amino alcohol and dinitriles (**4a**–**4c**) as substrates in chlorobenzene at reflux for 12 h (Table 1).

The results showed that both micro CPs **1** and **2** were efficient heterogeneous catalysts for the reaction of L-amino alcohol with dinitriles, giving **5a**–**5c** with moderate to high yields (68–86%) along with trace of bis-oxazoline products. Amazingly, mono-oxazolines were formed as the major products by using micro CPs **1** and **2** as the heterogeneous catalysts. In comparison, homogeneous catalyst $ZnCl_2$, which is a commonly used Lewis acid catalyst for the cyclization reaction, gave both the mono-oxazoline and bis-oxazoline cyclization products under the same reaction conditions (Table S1 in the SI). Only under a series of harsh conditions, such as long reaction times and water- and oxygen-free conditions, bis-oxazoline products could be obtained with yields ranging from 51–61% in 72 h.[28] When the same equivalent of H_3idbt ligand (0.1 mmol) was added under the same reaction conditions, no products could be obtained. The catalytically active sites are believed to the CPs **1** and **2**

In addition, inductively coupled plasma mass spectrometric (ICP-MS) analysis of the supernatant showed very little Zn leaching (≈1 ppm for **1** and ≈4 ppm for **2**) after the catalytic reactions. Next, we carried out a hot filtration experiment. After 18 or 25% conversion of **4a** in the presence of **1** or **2** in 1 h, the reaction mixture was passed through a sand core funnel to remove the catalysts, and the supernatant was allowed to stand for 11 h. It was found that the conversion of the supernatant remained almost unchanged during the process. Thus, these experiments unambiguously confirmed their heterogeneity.

To probe whether catalysis occurs inside the cavity or on the surface of the catalysts, a sterically demanding substrate biphenyl-4,4′-dicarbonitrile (**4d**) was subjected to the catalytic conditions. Consequently, a conversion of 47% and 60% (Table 1, entries 7 and 8) with micro CPs **1** and **2** as catalysts, respectively, was achieved. Because **4d** is difficult to diffuse into small cavities of **1** and **2**, the active sites on the surface of the catalysts are believed to catalyze the reaction.

We have also examined the catalytic activities of bulk crystals **1** (≈0.20×0.20×0.15 mm^3) or **2** (≈0.25×0.22×0.19 mm^3) for the cyclization reaction of **3** and **4a** without grinding and stirring to eliminate the possibility of catalytic activity resulting from the surface metal sites of very tiny particles. Less than 40% yield was observed after 12 h, which was much lower than the 83 and 86% yield obtained with microscale crystalline **1** and **2**, respectively. The result indicates that the cyclization reaction also occurs inside the framework at the same time because big crystals own too few surface metal sites to account for the catalytic reaction. Furthermore, the experimental Brunauer-Emmett-Teller (BET) surface area for the micro and bulk crystals was 194 and 9.2428 $m^2 g^{-1}$, which clearly shows that catalytic activities depend on the surface catalytic sites of particle sizes (Figure S4 in the SI). Therefore, these results provided evidence that the catalysis reactions for **4a**–**c** may take place on the surface and inside of the crystals with single-site catalysis.

The catalysts for the synthesis of mono-oxazolines could be evaluated from site-isolation. Due to their well-defined crystalline nature, a very valuable feature of CPs is that they can provide atomistically well-defined isolated active catalytic sites with uniformly fixed azimuth and distance throughout the solid, mimicking the site-isolation of many catalytic enzymes assemblies in nature. These identical isolated active sites can catalyze the reaction without synergistic interactions, selectively achieving mono-oxazolines from dinitrile compounds. As for **1**, Zn2 ions are isolated and have accessible active sites due to their unsaturated metal center. As for **2**, Zn3 ions are catalytically active sites. We speculate that one of the cyano groups is activated by the Zn Lewis active sites. Because there are no synergistic interactions in the active sites of **1** and **2**, the reactions lead to mono-oxazolines as the major products. Combined with high site density onto the complexes, the single-site isolation leads to high conversion. The mechanism for the synthesis of mono-oxazolines catalyzed by the Zn-based CPs had been proposed (Scheme 1). The dinitrile is first activated by the catalyst to give **I**. Then, L-amino alcohol attacks **I** to

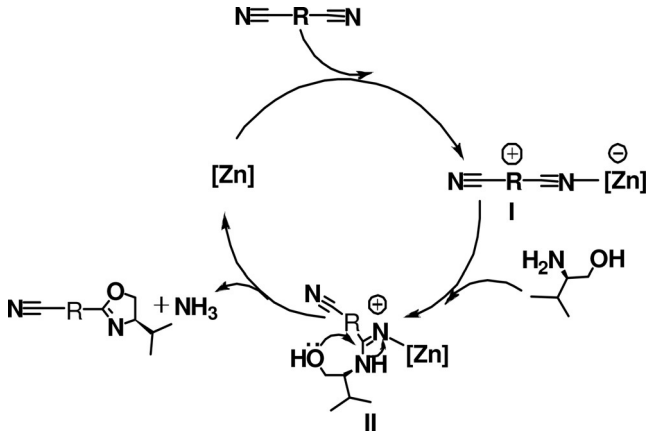

Scheme 1. Proposed mechanism for the synthesis of mono-oxazolines catalyzed by micro Zn-based CPs.

afford **II**. Cyclization of **II** gives the final product and releases the catalyst for the next catalytic cycle.

In addition, compared with the previous Lewis acid homogeneous catalyst for the cyclization reaction,[26,44] micro CPs **1**–**2** as heterogeneous catalysts could yield several principal advantages, such as high selectivity, reusability, easy separation, and environmental friendliness. Furthermore, we have also examined the recyclability and stability of **1**–**2** for the catalytic reaction with **4a**. In the recyclability experiments, catalysts **1**–**2** were readily recovered from the catalytic reaction by filtration, and could be recycled and reused at least five times (Figure S5 in the SI). Moreover, the PXRD patterns of the microcrystallites of **1**–**2** after the fifth catalytic reaction closely matched those of single crystals of **1**–**2** and showed no signs of framework collapse and decomposition, which indicates that the framework could remain intact after at least five cycles (Figure S6 in the SI).

Conclusions

In conclusion, by using tetrazole-appended imidazole (H_3idbt) as a rigid and conjugated clamp-like ligand, two catalytically active zinc(II)-based CPs were successfully obtained by the solvothermal reactions with good yields. In addition, their microcrystallines were successfully produced by hydrothermal methods in the presence of PVP-1300000, CTAB or SDS as surfactants. For both the micro CPs, as the surfactants concentration increased, their crystallite sizes could be scaled down to the micrometer regime. For the tandem condensation–cyclodehydration reaction of the amino alcohol and dinitriles, micro CPs **1** and **2** showed good catalytic ability for the selective synthesis of mono-oxazolines by virtue of their immobilizing well-defined catalytic sites. Moreover, they could be easily recovered by filtration and reused at least after five cycles without significant loss of yield. This approach provided a new strategy for the design of efficient heterogeneous catalysts for the selective synthesis of mono-oxazolines.

Experimental Section

Materials and physical measurements

All reagents and solvents were commercially available and used without any further purification, except for ligand H_3idbt, which was synthesized according to the literature.[45] Inductively coupled plasma spectra (ICP) were performed on a Thermo ICAP 6500 DUO spectrometer. The FTIR spectra were recorded in the region of 400–4000 cm^{-1} on a Bruker Tensor 27 spectrophotometer from KBr pellets. Elemental analysis was performed on a FLASH EA 1112 elemental analyzer. Powder X-ray diffraction (PXRD) patterns were recorded using $Cu_{K\alpha1}$ radiation on a PANalytical X'Pert PRO diffractometer. Thermogravimetric analyses (TGA) were implemented on a Netzsch STA 449C thermal analyzer and the samples were heated at a rate of 10 °C min^{-1} under air atmosphere. A Hitachi TM-1000 field emission scanning electron microscopy (SEM) was used to image the particles size and morphologies. The BET surface of crystal was collected on Micromeritics ASAP 2420 Accelerated Surface Area under ultrahigh vacuum in a clean system, with a diaphragm and turbo pumping system. Ultrahigh-purity-grade (> 99.999%) N_2 gas was applied in the adsorption measurements. The experimental temperature was maintained by liquid nitrogen (77 K). ^{1}H and ^{13}C NMR spectra were conducted on a Bruker Avance-400 spectrometers. High-resolution mass spectra (HRMS-ESI) were recorded with a Micro Q-TOF mass spectrometer.

Synthesis of $[\{Zn_6(idbt)_4(phen)_4\}\cdot 3\ H_2O]_n$ (1)

A mixture of $ZnSO_4$ (0.016 g, 0.10 mmol), H_3idbt (0.020 g, 0.10 mmol), and phen (0.020 g, 0.10 mmol) was dissolved in *N*,*N*′-dimethylformamide (DMF, 5 mL)/H_2O (3 mL) at room temperature. The reaction mixture was heated at 160 °C for 3 days in a 25 mL Teflon-lined stainless-steel autoclave. Upon cooling of the reactor to room temperature at a rate of 5 °C h^{-1}, filtration of the reaction mixture afforded colorless crystals. The products were filtered and collected (yield ≈36% based on Zn). Anal. Calcd (%) for $C_{68}H_{42}N_{48}O_3Zn_6$: C, 41.42; H, 2.15; N, 34.10. Found: C, 41.88; H, 2.03; N, 34.15. IR (KBr): $\tilde{\nu}$ = 3444 (s), 3060 (w), 3020 (w), 1136 (m), 1104 (m), 1026 (m), 728 (vs), 672 (w) cm^{-1}.

Synthesis of microcrystalline 1 in the presence of PVP-1300000

$ZnSO_4$ (0.032 g, 0.20 mmol), H_3idbt (0.040 g, 0.20 mmol), phen (0.040 g, 0.20 mmol), and PVP-1300 000 (0.15 g) were mixed in a solution of DMF/H_2O (5/3 mL) and stirred at room temperature for 0.5 h to obtain a uniform mixture. The reaction mixture was heated at 160 °C h^{-1} for 3 days in a 25 mL Teflon-lined stainless-steel autoclave. The reactor was cooled to room temperature at a rate of 5 °C h^{-1}. The microcrystalline of **1** were isolated by centrifugation and washing with ethanol and water (yield ≈33% based on Zn).

Synthesis of microcrystalline 1 in the presence of CTAB

The procedure is similar to that of microcrystalline **1** prepared with PVP-1 300 000, except that CTAB (0.15 g) was used instead of PVP-1 300 000 (0.15 g). The products were isolated and collected (yield ≈34% based on Zn).

Synthesis of microcrystalline 1 in the presence of SDS

The procedure is similar to that of microcrystalline **1** prepared with PVP-1 300 000, except that SDS (0.15 g) was used instead of PVP-

1 300 000 (0.15 g). The products were isolated and collected (yield ≈30% based on Zn).

Synthesis of $[\{Zn_3(idbt)_2(H_2O)_4\}\cdot 2H_2O]_n$ (2)

A mixture of $Zn(NO_3)_2$ (0.019 g, 0.10 mmol) and H_3idbt (0.010 g, 0.05 mmol) was dissolved in EtOH (4 mL) and $NH_3\cdot H_2O$ (4 mL) at room temperature. The reaction mixture was heated at 130 °C for 3 days in a 25 mL Teflon-lined stainless-steel autoclave. Upon cooling of the reactor to room temperature at a rate of 5 °C h^{-1}, filtration of the reaction mixture afforded colorless crystals. The products were filtered and collected (yield ≈45% based on Zn). Anal. Calcd (%) for $C_{10}H_{14}N_{20}O_6Zn_3$: C, 16.98; H, 2.00; N, 39.63. Found: C, 16.81; H, 2.10; N, 39.52. IR (KBr): $\tilde{\nu}$ = 3337 (w), 3169 (w), 1559 (m), 1272 (m), 1245 (m), 1131 (s), 992 (vs), 695 (s), 665 (vs) cm^{-1}.

Synthesis of microcrystalline 2 in the presence of PVP-1300 000

A mixture of $Zn(NO_3)_2\cdot 6H_2O$ (0.038 g, 0.20 mmol), H_3idbt (0.020 g, 0.10 mmol), and PVP-1300 000 (0.15 g) was added into a 25 mL Teflon-lined stainless steel vessel. Then, 4 mL ethanol solution was added. The reaction mixture was stirred at room temperature for 0.5 h. After that, 4 mL $NH_3\cdot H_2O$ was added and stirred at room temperature for another 10 min. The reaction mixture was kept in a 25 mL Teflon-lined stainless steel vessel at 130 °C for 3 days. After cooling, the reaction system was isolated by centrifuging and washed with ethanol and water to remove the supernatant (yield ≈42% based on Zn).

Synthesis of microcrystalline 2 in the presence of CTAB

The procedure is similar to that of microcrystalline **2** prepared with PVP-1 300 000, except that CTAB (0.15 g) was used instead of PVP-1 300 000 (0.15 g). The products were isolated and collected (yield ≈44% based on Zn).

Synthesis of microcrystalline 2 in the presence of SDS

The procedure is similar to that of microcrystalline **2** prepared with PVP-1300 000, except that SDS (0.15 g) was used instead of PVP-1300 000 (0.15 g). The products were isolated and collected (yield ≈42% based on Zn).

Typical procedure for the synthesis of mono-oxazolines (5a–d) with microscale catalysts 1 and 2

Nitrile (1.0 mmol, **4a–d**), L-amino alcohol (3.0 mmol), microscale catalysts **1** and **2** (0.1 mmol, 0.1 equiv based on zinc ion), and chlorobenzene (5 mL) were mixed and heated to reflux. The mixture was stirred at reflux for approximately 12 h. After completion of the reaction, the mixture was diluted with ethyl acetate. The product was then filtered and extracted with brine. The organic phase was dried with Na_2SO_4. Evaporation of the organic phase and purification of the crude product by column chromatography on silica gel gave the pure product.

Catalyst recycling experiments

To evaluate the stability of the solid catalysts, we investigated recycled and reused **1** and **2** in the reaction. After the 1st run, the catalysts were separated by centrifugation and then washed with ethyl acetate (EtOAc) to remove adsorbed organic substrates, followed by drying overnight at room temperature to be reused. The catalysts were used for the 2nd run without further activation, and the same processes were repeated for the next run.

Crystal data collection and refinement

The data of complex **1** was collected on a SuperNova diffractometer with graphite monochromated $Cu_{K\alpha}$ radiation (λ = 1.54178 Å) at 293(2) K, whereas the data of complex **2** was collected on a Rigaku Saturn 724 CCD diffractometer with $Mo_{K\alpha}$ radiation (λ = 0.71073 Å) at 293(2) K. Absorption corrections were applied by using a numerical program. The data were modified for Lorentz and polarization effects. The structures were determined by immediate methods and refined with a full-matrix least-squares technique based on F^2 with the SHELXL-97 crystallographic software package.[46] Hydrogen atoms were placed at calculated positions and refined as riding atoms with isotropic displacement parameters. Crystallographic data and structure processing parameters for **1** and **2** are summarized in Table S2 in the Supporting Information. Selected bond lengths and bond angles of **1** and **2** are listed in Table S3 of the Supporting Information. CCDC 1439274 (**1**), and 1439275 (**2**) contain the supplementary crystallographic data for this paper. These data can be obtained free of charge from The Cambridge Crystallographic Data Centre.

Acknowledgements

This work was funded by the National Natural Science Foundation (Nos. 21201152; 21371155), Research Fund for the Doctoral Program of Higher Education of China (20124101110002), and the Student Innovative Funded Projects of Zhengzhou University (201510459049).

Keywords: heterogeneous catalysis · microcrystallines · oxazolines · polymers · surfactants

[1] L. J. Murray, M. Dincă, J. R. Long, *Chem. Soc. Rev.* **2009**, *38*, 1294–1314.
[2] O. K. Farha, A. O. Yazaydin, I. Eryazici, C. D. Malliakas, B. G. Hauser, M. G. Kanatzidis, S. T. Nguyen, R. Q. Snurr, J. T. Hupp, *Nat. Chem.* **2010**, *2*, 944–948.
[3] H. Furukawa, N. Ko, Y. B. Go, N. Aratani, S. B. Choi, E. Choi, A. O. Yazaydin, R. Q. Snurr, M. O'Keeffe, J. Kim, O. M. Yaghi, *Science* **2010**, *329*, 424–428.
[4] L. X. Sun, L. F. Song, C. H. Jiang, C. L. Jiao, J. A. Zhang, F. Xu, W. S. You, Z. G. Wang, J. J. Zhao, *Cryst. Growth Des.* **2010**, *10*, 5020–5030.
[5] S. Achmann, G. Hagen, J. Kita, I. M. Malkowsky, C. Kiener, R. Moos, *Sensors* **2009**, *9*, 1574–1589.
[6] R. E. Morris, A. C. McKinlay, P. Horcajada, G. Férey, R. Gref, P. Couvreur, C. Serre, *Angew. Chem. Int. Ed.* **2010**, *49*, 6260–6266; *Angew. Chem.* **2010**, *122*, 6400–6406.
[7] C. A. Kent, D. Liu, L. Ma, J. M. Papanikolas, T. J. Meyer, W. Lin, *J. Am. Chem. Soc.* **2011**, *133*, 12940–12943.
[8] C. Y. Lee, O. K. Farha, B. J. Hong, A. A. Sarjeant, S. T. Nguyen, J. T. Hupp, *J. Am. Chem. Soc.* **2011**, *133*, 15858–15861.
[9] J. Lee, O. K. Farha, J. Roberts, K. A. Scheidt, S. T. Nguyen, J. T. Hupp, *Chem. Soc. Rev.* **2009**, *38*, 1450–1459.
[10] A. Dhakshinamoorthy, M. Alvaro, H. Garcia, *Chem. Commun.* **2010**, *46*, 6476–6478.
[11] A. Dhakshinamoorthy, M. Alvaro, P. Horcajada, E. Gibson, M. Vishnuvarthan, A. Vimont, J. Grenèche, C. Serre, M. Daturi, H. Garcia, *ACS Catal.* **2012**, *2*, 2060–2065.
[12] S. Horike, M. Dincă, K. Tamaki, J. R. Long, *J. Am. Chem. Soc.* **2008**, *130*, 5854–5855.
[13] J. M. Roberts, B. M. Fini, A. A. Sarjeant, O. K. Farha, J. T. Hupp, K. A. Scheidt, *J. Am. Chem. Soc.* **2012**, *134*, 3334–3337.

[14] F. Song, C. Wang, J. M. Falkowski, L. Ma, W. Lin, *J. Am. Chem. Soc.* **2010**, *132*, 15390 – 15398.
[15] S. Cho, B. Ma, S. T. Nguyen, J. T. Hupp, T. E. Albrecht-Schmitt, *Chem. Commun.* **2006**, 2563 – 2565.
[16] W. Zhang, W. Gao, Pham, T. P. Jiang, S. Ma, *Cryst. Growth Des.* **2016**, *16*, 1005 – 1009.
[17] F. Carson, S. Agrawal, M. Gustafsson, A. Bartoszewicz, F. Moraga, X. Zou, B. Martín-Matute, *Chem. Eur. J.* **2012**, *18*, 15337 – 15344.
[18] M. Tonigold, Y. Liu, A. Mavrandonakis, A. Puls, R. Staudt, J. Möllmer, J. Sauer, D. Volkmer, *Chem. Eur. J.* **2011**, *17*, 8671 – 8695.
[19] C. Huang, R. Ding, C. Song, J. Lu, L. Liu, X. Han, J. Wu, H. Hou, Y. Fan, *Chem. Eur. J.* **2014**, *20*, 16156 – 16163.
[20] R. Ding, C. Huang, J. Lu, J. Wang, C. Song, J. Wu, H. Hou, Y. Fan, *Inorg. Chem.* **2015**, *54*, 1405 – 1413.
[21] B. Li, K. Leng, Y. Zhang, J. J. Dynes, J. Wang, Y. Hu, D. Ma, Z. Shi, L. Zhu, D. Zhang, Y. Sun, M. Chrzanowski, S. Ma, *J. Am. Chem. Soc.* **2015**, *137*, 4243 – 4248.
[22] F. Rondu, G. L. Bihan, X. Wang, A. Lamouri, E. Touboul, G. Dive, T. Bellahsene, B. Pfeiffer, P. Renard, B. Guardiola-Lemaıtre, D. Manéchez, L. Pénicaud, A. Ktorza, J. J. Godfroid, *J. Med. Chem.* **1997**, *40*, 3793 – 3803.
[23] P. Bousquet, J. Feldman, *Drugs* **1999**, *58*, 799 – 812.
[24] E. S. Vizi, *Med. Res. Rev.* **1986**, *6*, 431 – 449.
[25] P. Wipf, P. C. Fritch, *Tetrahedron Lett.* **1994**, *35*, 5397 – 5400.
[26] C. Bolm, K. Weickhardt, M. Zehnder, T. Ranff, *Chem. Ber.* **1991**, *124*, 1173 – 1180.
[27] M. Gómez, S. Jansat, G. Muller, M. A. Maestro, J. M. Saavedra, M. Font-Bardía, X. S. Font-Bardía, *J. Chem. Soc. Dalton Trans.* **2001**, 1432 – 1439.
[28] M. Luo, J. Zhang, J. Sun, S. Zhou, H. Yin, K. Hu, *J. Comb. Chem.* **2009**, *11*, 220 – 227.
[29] H. C. Aspinall, O. Beckingham, M. D. Farrar, N. Greeves, C. D. Thomas, *Tetrahedron Lett.* **2011**, *52*, 5120 – 5123.
[30] I. Mohammadpoor-Baltork, V. Mirkhani, M. Moghadam, S. Tangestaninejad, M. A. Zolffiol, M. Abdollahi-Alibeik, A. R. Khosropour, H. Kargar, S. F. Hojati, *Catal. Commun.* **2008**, *9*, 894 – 901.
[31] R. Rasappan, D. Laventine, O. Reiser, *Coord. Chem. Rev.* **2008**, *252*, 702 – 714.
[32] T. Ohshima, T. Iwaski, K. Mashima, *Chem. Commun.* **2006**, 2711 – 2713.
[33] M. Moghadam, V. Mirkhani, S. Tangestaninejad, I. Mohammadpoor-Baltork, H. J. Kargar, *Iran. Chem. Soc.* **2009**, *6*, 251 – 258.
[34] W. Lin, W. J. Rieter, K. M. L. Taylor, *Angew. Chem. Int. Ed.* **2009**, *48*, 650 – 658; *Angew. Chem.* **2009**, *121*, 660 – 668.
[35] A. Dhakshinamoorthy, M. Alvaro, Y. K. Hwang, Y. K. Seo, A. Corma, H. Garcia, *Dalton Trans.* **2011**, *40*, 10719 – 10724.
[36] J. Hermannsdörfer, M. Friedrich, R. Kempe, *Chem. Eur. J.* **2013**, *19*, 13652 – 13657.
[37] L. Liu, Z. B. Han, S. M. Wang, D. Q. Yuan, S. W. Ng, *Inorg. Chem.* **2015**, *54*, 3719 – 3721.
[38] M. S. Bakshi, F. Possmayer, N. O. Petersen, *Chem. Mater.* **2007**, *19*, 1257 – 1266.
[39] S. Banerjee, K. Loza, W. Meyer-Zaika, O. Prymak, M. Epple, *Chem. Mater.* **2014**, *26*, 951 – 957.
[40] R. J. Bergeron, *Chem. Rev.* **1984**, *84*, 587 – 602.
[41] R. S. Roy, A. M. Gehring, J. C. Milne, P. J. Belshaw, C. T. Walsh, *Nat. Prod. Rep.* **1999**, *16*, 249 – 263.
[42] J. R. Lewis, *Nat. Prod. Rep.* **2002**, *19*, 223 – 258.
[43] Z. Jin, *Nat. Prod. Rep.* **2003**, *20*, 584 – 605.
[44] M. Luo, X. Li, Y. Ke, H. Yin, K. Hu, J. Zhang, *Heteroat. Chem.* **2007**, *18*, 679 – 683.
[45] M. Dincă, T. David Harris, A. T. Iavarone, J. R. Long, *J. Mol. Struct.* **2008**, *890*, 139 – 143.
[46] G. M. Sheldrick, *Acta Crystallogr. Sect. A* **2008**, *64*, 112 – 122.

Manuscript received: March 29, 2016
Accepted Article published: May 2, 2016
Final Article published: May 24, 2016